Anatomy of a strong and prolonged Rio Grande Rift earthquake swarm

Alan R. Sanford and Hans E. Hartse
2016, pp. 225-233. https://doi.org/10.56577/FFC-67.225

in:

Guidebook 67 - Geology of the Belen Area, Frey, Bonnie A.; Karlstrom, Karl E. ; Lucas, Spencer G.; Williams, Shannon; Zeigler, Kate; McLemore, Virginia; Ulmer-Scholle, Dana S., New Mexico Geological Society 67th Annual Fall Field Conference Guidebook, 512 p. https://doi.org/10.56577/FFC-67

This page is intentionally left blank to maintain order of facing pages.

New Mexico Geological Society Guidebook, 67th Field Conference, Geology of the Belen Area, 2016, p. 225-233.

ANATOMY OF A STRONG AND PROLONGED RIO GRANDE RIFT EARTHQUAKE SWARM

Allan R. Sanford[1], and Hans E. Hartse[2]

[1]Emeritus Professor of Geophysics, Earth and Environmental Sciences Department, New Mexico Tech, Socorro, NM 87801;
[2]Geophysics Group, Los Alamos National Laboratory, Los Alamos, NM (hartseatlanl.gov)

Abstract—Between November 1989 and June 1991, a strong earthquake swarm near Bernardo, New Mexico occurred within the Rio Grande rift. Using data from their short-period seismograph network, temporarily deployed seismic stations, and other regional seismic data, researchers at New Mexico Tech observed four earthquakes of between duration magnitude 4.1 and 4.7 (all felt in Socorro), and many additional smaller earthquakes. The Gutenberg-Richter relationship between earthquake frequency and magnitude for the swarm has a b-value of 0.57, or fewer small events relative to the numbers of large events than is typically observed for tectonic areas (where b-values are close to 1). The best-constrained aftershock locations following the two largest events cover epicentral areas of between 4 and 4.5 km^2, with depths ranging between 4 and 6.5 km. Aftershock trends, focal mechanism solutions from first motions, and modeling of regional broadband data conducted by other researchers suggest the swarm occurred along adjacent, nearly parallel normal faults with strikes trending slightly east of north. The events occurred just above a west-to-east trending listric fault previously imaged on active-source crustal profiles obtained in the Bernardo area. Thus, a triggering mechanism for the Bernardo swarm may be aseismic movement on the east-trending listric fault stressing north-trending normal faults in the shallower crust above.

INTRODUCTION

An earthquake swarm of approximately 19 months duration, from 8 November 1989 to 22 June 1991, and centered at 34°27.0'N by 106°52.5'W near Bernardo, New Mexico, occurred within an active zone of crustal extension in the Rio Grande rift (RGR) (Morgan et al., 1986; Keller and Baldridge, 1999; Fig. 1). Earthquakes within this rift have produced nearly all the strong historical earthquakes in New Mexico (Sanford et al., 2002, 2006). Prior to 1962, when instrumental recording began, strong (felt) earthquakes appear to have occurred towards the central part of the rift rather than its margins. All strong RGR earthquakes since 1962 also have been located toward the central part of the rift, including the 1989-1991 Bernardo swarm that produced shocks of magnitude 4.7, 4.6, 4.1, and 4.3 over its first 12 months. These events represent 50 percent of the earthquakes greater than magnitude 4.0 in the New Mexico segment of the RGR since 1962.

The swarm occurred within the boundary of the Socorro Seismic Anomaly (SSA), an unusually high seismicity region feature of the RGR in New Mexico (Sanford et al., 1995) (Fig. 2). Seismicity within this ~5000 km^2 area is the highest of any region in the entire state (Sanford et al., 2002). The SSA is centered over the Socorro Magma Body, a sill of about 3400 km^2 approximately 150 m thick at a depth of 18.75 km (Balch et al., 1997; Ake and Sanford, 1988; Hartse et al., 1992). Surface uplift that is believed to be the result of inflation of this mid-crustal magma body reaches a maximum of ~3 mm a year about 16 km south of the swarm (Reilinger and Oliver, 1976; Fialko and Simmons, 2001).

The location of the 1989-91 swarm is fortuitous, as it occurred within a few kilometers of two east-west oriented, high resolution seismic reflection profiles (Brown et al., 1980; Russell and Snelson, 1994) (Fig. 3). The existence of these profiles allowed the establishment of relationships between swarm hypocenter distributions and prominent subsurface faults.

EARTHQUAKE DATA RECORDING AND INTERPRETATION

Acquisition of Swarm Data

Earthquakes in the 1989-91 swarm were recorded by the telemetered New Mexico Tech (NMT) seismograph network centered on Socorro in the RGR (Fig. 2). At the time of the swarm, nine stations of this network were in operation, with the three nearest stations at distances of ~5-7 km, ~24-26 km, and ~26-28

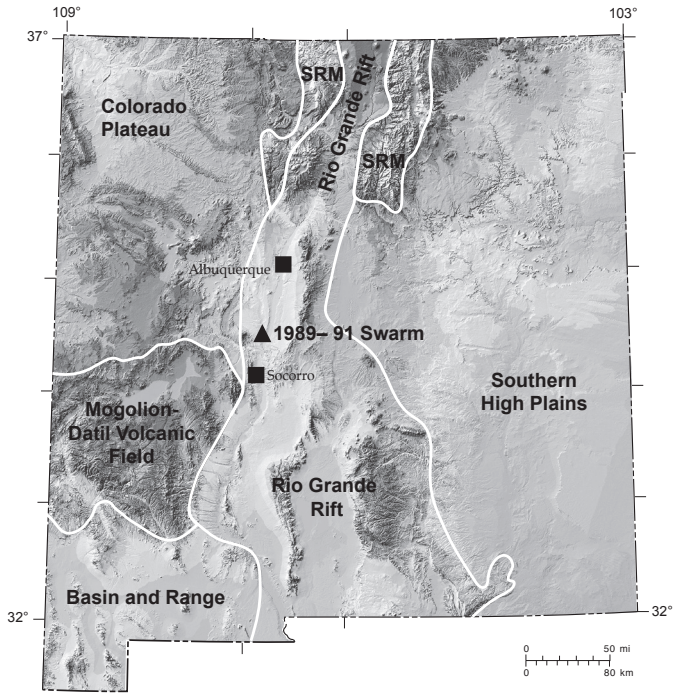

FIGURE 1. Physiographic provinces of New Mexico showing the 1989-1991 earthquake swarm in the Rio Grande rift.

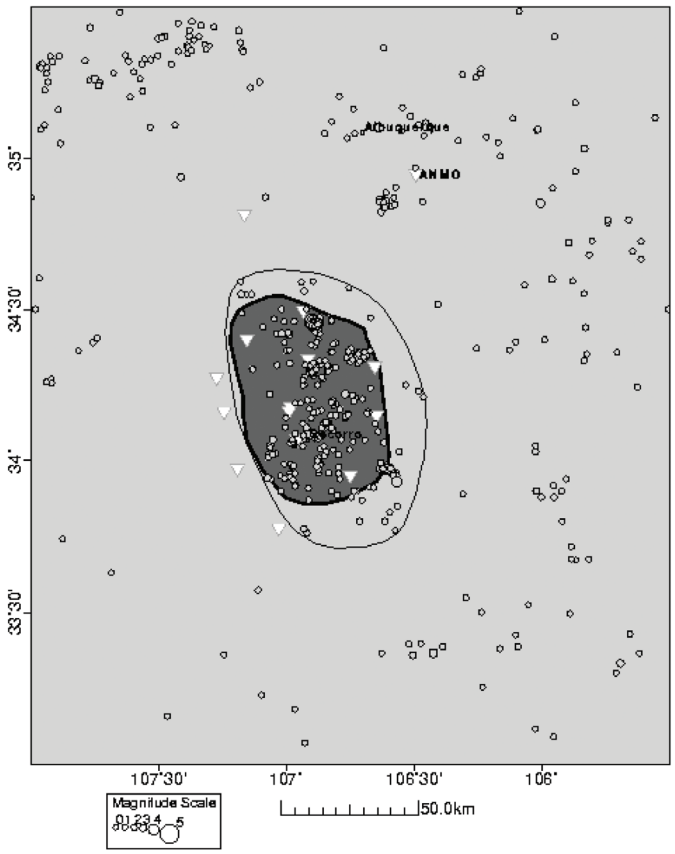

FIGURE 2. Earthquake epicenters (M≥1.3) from 1962-1995 defining the Socorro Seismic Anomaly (largest elliptical area outlined). The darer, smaller elliptical area is the mapped extent of the Socorro Magma Body (Sanford et al., 1995; Balch et al., 1997). Triangle symbols indicate the location of permanent stations in the NMT seismograph network.

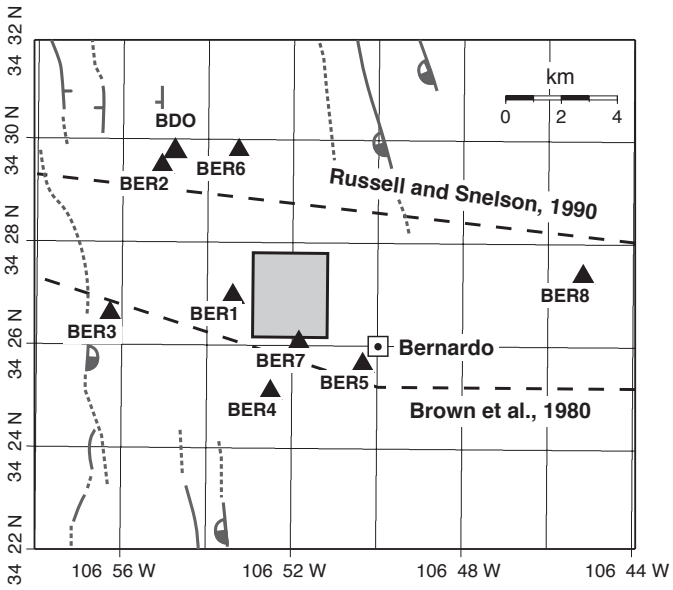

FIGURE 3. Location of seismic reflection profiles relative to the 1989-1991 swarm; the approximately seven km^2 region NW of Bernardo. Also shown are locations of temporary seismograph stations and mapped surface faults (Machette et al., 1998).

km. The nearest station, BDO (Fig. 3), was not installed and operational until late February 1990, three months after the beginning of the swarm. Arrival times, signal durations, and direction of first motions from the NMT network were the primary data used to establish hypocenters, magnitudes, and earthquake focal mechanisms. For short periods after the strong shocks (M≥4.1), one to three temporary stations were placed at distances of approximately 2 to 12 km from the center of the swarm (Fig. 3). The most accurate hypocenters for the events in the swarm were obtained when the temporary stations were deployed.

The NMT network data were recorded by 1 Hz short-period, vertical seismometers. Analog radio telemetry was used to transmit the data to the NMT central recording facility where it was written on helicorder recorders at 1 mm/s. The temporary stations also used 1-Hz short-period seismometers but data was recorded in the field on smoked-paper helicorders at 2 mm/s. ALQ and ANMO data were recorded digitally with data now archived at the IRIS Data Management Center.

Magnitudes

All magnitudes in this report on the 1989-91 earthquake swarm are duration magnitudes obtained from the relationship:

$$Md = 2.79 \log Td - 3.63,$$

in which Td is the duration of the earthquake recording in seconds on ALQ – WWSN seismograms or on seismograms produced by instruments with similar frequency responses and magnifications. This relationship was first developed for New Mexico earthquakes at Los Alamos National Laboratory (Newton et al., 1976). Later, an essentially similar relationship for New Mexico earthquakes was derived at the New Mexico Institute of Mining and Technology (Ake et al., 1983).

Time History of the Bernardo Swarm

The temporal distribution of earthquakes for the 572-day duration of the swarm is shown in Figure 4. The 117 events used for the figure is complete for all earthquakes of magnitude 1.3 or greater. Not shown in the figure is a single foreshock of magnitude 1.4 from 18 November 1989, 11 days before the swarm began at 0654 (all reported origin times are GMT) on 29 November 1989. The four strongest shocks, all of which were felt in Socorro, had magnitudes of 4.7, 4.6, 4.1 and 4.3 and were distributed as follows: M=4.7 at the beginning of the swarm, M=4.6 and M=4.1 on days 62 and 63 of the swarm, and M=4.3 on the day 345. The four shocks account for 96 % of the total seismic moment of the swarm (3.15 x 10^{16} Nm). The aftershocks in the 10-day intervals following the occurrence of the four strongest quakes produced nearly 40 % of the shocks of magnitude 1.3 or greater.

Important features of the time history are: (1) no single outstanding earthquake during the swarm; and (2) strong shocks at the beginning and end of the swarm.

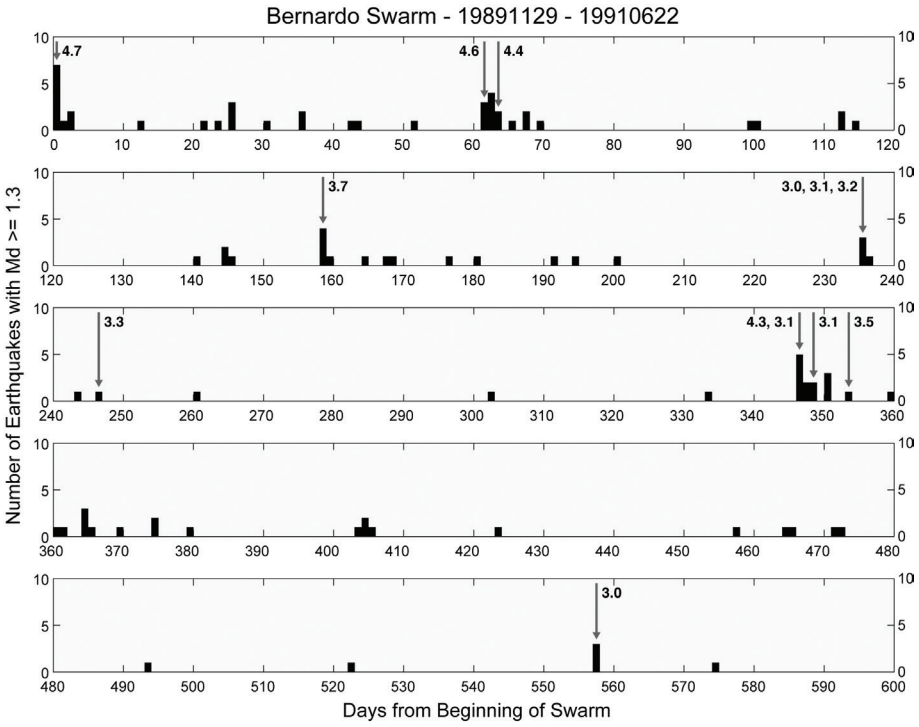

FIGURE 4. Time history of the 1989-1991 swarm. Plotted is the daily number of earthquakes of M≥1.3 for the 572-day duration of the swarm. First day of the swarm is November 29, 1989, when the largest earthquake of the sequence (Md = 4.73 occurred).

Earthquake Frequency Versus Magnitude

The Gutenberg-Richter (G-R) relationship between earthquake frequency and magnitude (Richter, 1958) is:

$$\text{Log}_{10} \sum N = a - bM,$$

in which $\sum N$ = the number of earthquakes of magnitude M or greater,

a = the $\log_{10}$ of the number of earthquakes with $M \geq 0$, and

b = the $\log_{10}$ of the increase in number of shocks for unit decrease in M.

The G-R relationship for the 117 shocks with $M \geq 1.3$ that occurred in the 571 days from the beginning of the swarm 29 November 1989 to its assumed end on 22 June 1991 is:

$$\text{Log}_{10} \sum N = 2.79 - 0.57M.$$

The b-value of 0.57 is based on the slope of a line from M=1.3 to M~3.7 (Fig. 5). An observation that suggests this is a robust number for the 1989-91 swarm is that an extrapolation to higher magnitudes yields four quakes of 4.74, 4.58, 4.32, and 4.12. This in good agreement with the observed strengths of the four strongest quakes in the swarm.

Epicenters and Focal Depths

Procedure

Earthquake origin times, epicenters, and focal depths were obtained using the inverse method computer program SEISMOS (Hartse, 1991). This location program was developed to utilize not only direct P and S arrivals but also reflection phases PzP, SzS, and SzP from the Socorro Magma Body (SMB) as shown in Figure 6. Hartse (1991) was able to demonstrate a reduction in focal depth error by a factor of ~3 when reflection phases were used in the locations. He was also able to simultaneously solve for hypocenters and a crustal velocity model to the depth of the magma body (~18.75 km) for the Socorro area (Fig. 6).

Hartse (1991) determined a set of station corrections for a general suite of earthquakes spread across the entire Socorro area. For the Bernardo swarm, a special set of station corrections was computed that minimized travel time residuals between the Bernardo hypocenters and the permanent and temporary recording stations.

M ≥ 4.1 Swarm Earthquakes

Listed in Table 1 are SEISMOS-determined latitude and longitudes for the epicenters of the four swarm earthquakes with $M \geq 4.1$. Also listed in Table 1 are origin times, magnitudes, and the number of duration measurements made. Arrival times at eight to nine stations of the NMT network (Fig. 2) and the USGS station ALQ approximately 65 km north were used for the SEISMOS epicenters. For one earthquake, 31 January 1990, P arrival times were available from two temporary stations (Fig. 3) within ~7 km of the epicenter. A focal depth of 6.03 km with a 1 s.d. error of 0.74 km was calculated for this shock.

Special Aftershocks Studies—M ≤ 0.7

For short periods of time following the earthquakes of magnitude 4.1 or greater, two or more temporary stations were

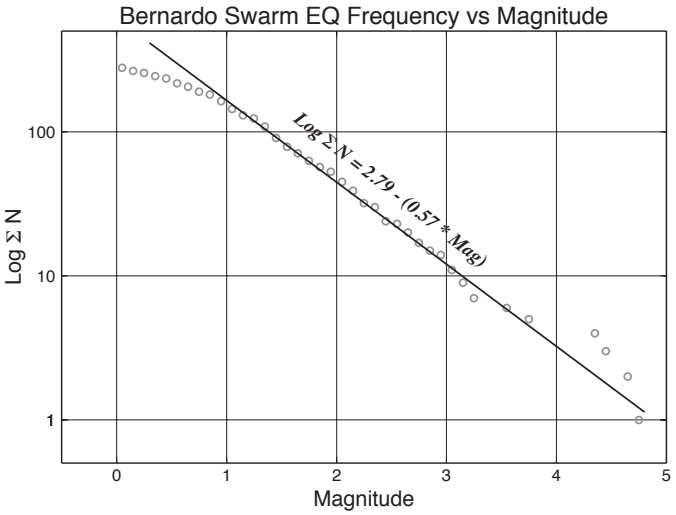

FIGURE 5. Earthquake frequency versus magnitude for the 1989-1991 swarm. Graph is based on the 117 swarm earthquakes of M≥1.3.

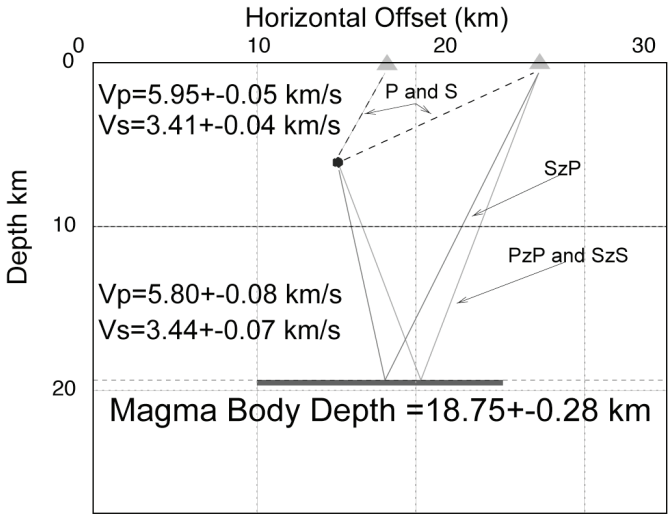

FIGURE 6. Velocity model and sample ray paths for a hypothetical earthquake. Triangles indicate seismic stations, and the reflecting layer represents the Socorro Magma Body. For details on the inversion that produced the crustal model, see Hartse et al. (1992).

deployed close to the epicenter area of the swarm. Only two of these deployments yielded sufficient data for analyses: (1) From 30 Nov. 1989 at 01:37 to 1 Dec. 1989 at 17:39 following the M=4.7 quake, and (2) From 30 Jan. 1990 at 00:24 to 1 Feb. 1990 at 15:02 following the M=4.6 quake. Because reflection phases from the SMB are most clearly defined on recordings of weak aftershocks by stations in the permanent NMT network, the analyzed data were restricted to events of $M \leq 0.7$. Hence, in the location process, inclusion of the reflected arrivals, nearly always SzP and SzS, yielded well-constrained focal depths in the location process, while the direct P phase arrivals from the very close temporary stations constrained the epicenters.

Epicenters, focal depths and cross-sections are presented in Figure 7 (Color Plate 10) for the recorded aftershocks of the M=4.7 earthquake on 29 Nov. 1989; and in Figure 8 (Color Plate 11) for the recorded aftershocks of the M=4.6 earthquake on 29 Jan. 1990. Table 2 lists numbers of aftershocks and average errors in depths, latitudes, and longitudes for the two aftershock studies.

If the assumption is made that nearly all recorded aftershocks are the result of breaching of small barriers remaining on the rupture surfaces, or triggered small events very near those surfaces, then the distribution of aftershocks may provide estimates of the (1) strikes and dips and (2) areas and shapes of the slip surfaces of the quakes. Presented below are estimates of these parameters for the strong shocks on 29 Nov. 1989 and 29 Jan. 1990 based on the distributions of small aftershocks.

30 Nov 1989 – 01 Dec 1989 Aftershocks

Strike. The distribution of epicenters in Figure 7a suggests a north strike to the slip surface of the M=4.7 quake. If the maverick event to the SE in this figure is discarded, the cross-sections in Figure 7b support a north strike. Note that the minimum lateral extent of the hypocenters is on the W-to-E cross section and the maximum on the S-to-N cross section.

Dip. The direction of dip cannot be determined from the distribution of hypocenters in the W-to-E cross section in Figure 7b because of the errors in latitude and longitude, but the distribution does indicate the dip must be quite steep.

Area of Activity. The distribution of hypocenters in the S-to-N cross section in Figure 7b encloses an area of ~4.5 km^2, a reasonable estimate of the extent of rupture for the M=4.7 shock.

30 Jan 1990 – 01 Feb 1990 Aftershocks

Interpretation of the aftershocks recorded after the M=4.6 earthquake may possibly be affected by some aftershocks of the earlier M=4.7, but the time history (Fig. 4) indicates these events should be very rare. In the interpretations that follow, all aftershocks recorded after the 29 Jan. 1990 quake are assumed to be on a very near but different slip surface than the 29 Nov. 1989 quake. Also note that although the relatively strong M=4.1 event on 31 Jan. 1990 and its one small aftershock appear in Figures 8a and 8b, they are not considered in the interpretations.

Strike. The distribution of small aftershock epicenters in Figure 8a suggests a north strike to the slip surface of the M=4.6 quake, but the cross sections in Figure 8b may not support that direction. The similar extent of hypocenters on the S to N and S30W-to-N30E cross sections may indicate a midway strike of ~N15E. Although the minimum lateral extent of hypocenters is on the W-to-E cross section, it is only slightly less than the lateral extent on the S60E-to-N60W cross section, an observation that also supports a strike of ~N15E.

Dip. Direction of dip cannot be determined from the distributions of hypocenters in W-to-E and S60E-to-N60W cross sections because of location errors.

Area of Activity. The areas covered by aftershocks in the S-to-N and SW-to-NE cross sections in Figure 8b are ~4.0 km^2, a reasonable estimate of the extent of faulting for a M=4.6 earthquake.

TABLE 1. Four largest events of the Bernardo earthquake sequence.

Date Yr/Mo/Day	Magnitude Md (N)[1]	Origin Time (GMT, 1 sd in sec)	Latitude (d m N) (1 sd in km)	Longitude (d m W) (1 sd in km)
89/11/29	4.73 (8)	06:54:38.86 (0.08)	34 27.33 (0.76)	106 52.68 (0.28)
90/01/29	4.60 (8)	13:16:11.01 (0.07)	34 27.09 (0.65)	106 52.45 (0.33)
90/01/31	4.10 (4)	01:08:19.71 (0.07)	34 27.57 (0.41)	106 51.34 (0.35)
90/11/08	4.31 (9)	10:46:53.97 (0.10)	34 26.24 (0.56)	106 51.83 (0.31)

[1]N = number of stations used to estimate duration magnitude
sd = standard deviation

Aftershocks Summary

The small aftershocks of the M=4.7 and M=4.6 events indicate that these strong swarm shocks were produced by slip on two closely spaced, north-striking and, likely, steeply-dipping faults. Movements occurred over approximately

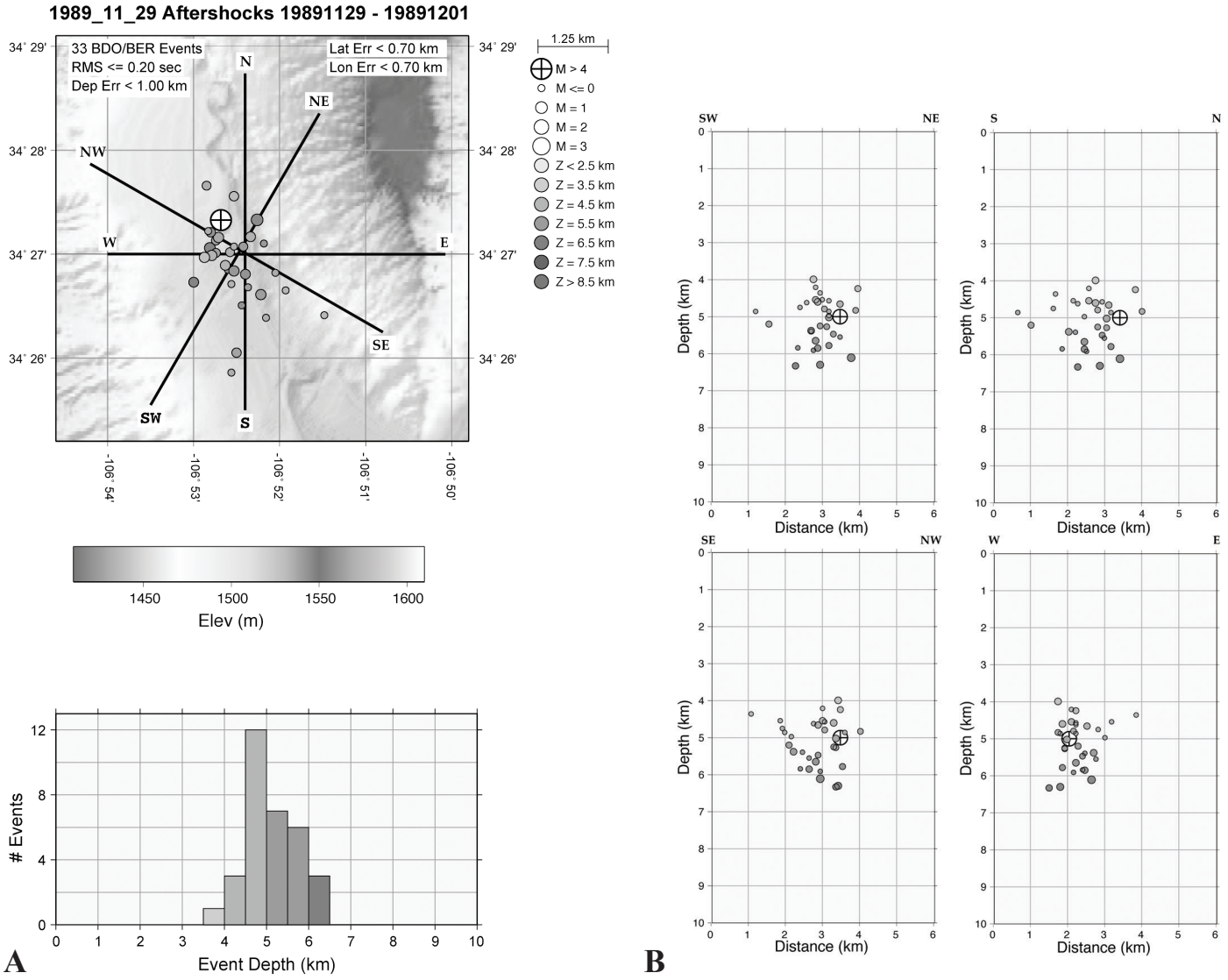

FIGURE 7. Aftershocks (M ≤ 0.7) of the 29 November 1989 M=4.7 earthquake. **A**) Epicenter map and focal depth historgram. **B**) Depth cross-sections. See also Color Plate 10.

the same depth interval, ~4 km to ~6.5 km, over areas of ~4.5 km^2 (M=4.7) and ~4.0 km^2 (M=4.6).

These results are consistent with Fan and Wallace (1991), who used broadband data from station ANMO (Albuquerque), 65 km north of the 1989-1991 swarm, to establish closely spaced north-striking faulting during the M=4.7 event on 29 Nov. 1989 and the M=4.6 event on 29 Jan. 1990. However, the Fan and Wallace focal depths were too strongly crustal model dependent to obtain good estimates of the depth parameter.

Fault Mechanisms From P-Wave First Motions

Fault-plane solutions were obtained for the two strongest earthquakes in the 1989-1991 swarm using directions of P-wave first motions within the computer program FPFIT (Reasenberg and Oppenheimer, 1985). A three layer crustal model was adopted for the fault mechanism determinations: (1) 5.88 km/s from 0 to 18.7 km; (2) 6.40 km/s from 18.7 km to 39.7 km; and (3) 8.00 km/s below 39.7 km. The model is based on the work of Hartse (1991) and the results of six seismic refraction surveys near Socorro that produced similar values for the depth (36.7±2.3 km) and velocity (7.95±0.19 km/s) of the Moho crustal discontinuity.

FPFIT diagrams of the two fault mechanisms are given in Figures 9 and 10, and parameters for the fault-plane solutions are listed in Table 3. First motions used in these solutions are from New Mexico Tech, Los Alamos National Laboratory, and the University of Texas-El Paso stations augmented by additional readings from stations in the published USGS locations for the two strongest shocks in the swarm. The first thing to note in the figures and table is that the T axis is nearly the same for the two earthquakes. However, the program FPFIT assigns the fault plane to the west-dipping nodal plane for the earthquake on 29 November 1989, and the fault plane to the east-dipping nodal plane for the earthquake on 29 January 1990. (Note that the parameter errors listed in Table 3 are 90% confidence interval errors for the nodal planes selected as the fault planes.)

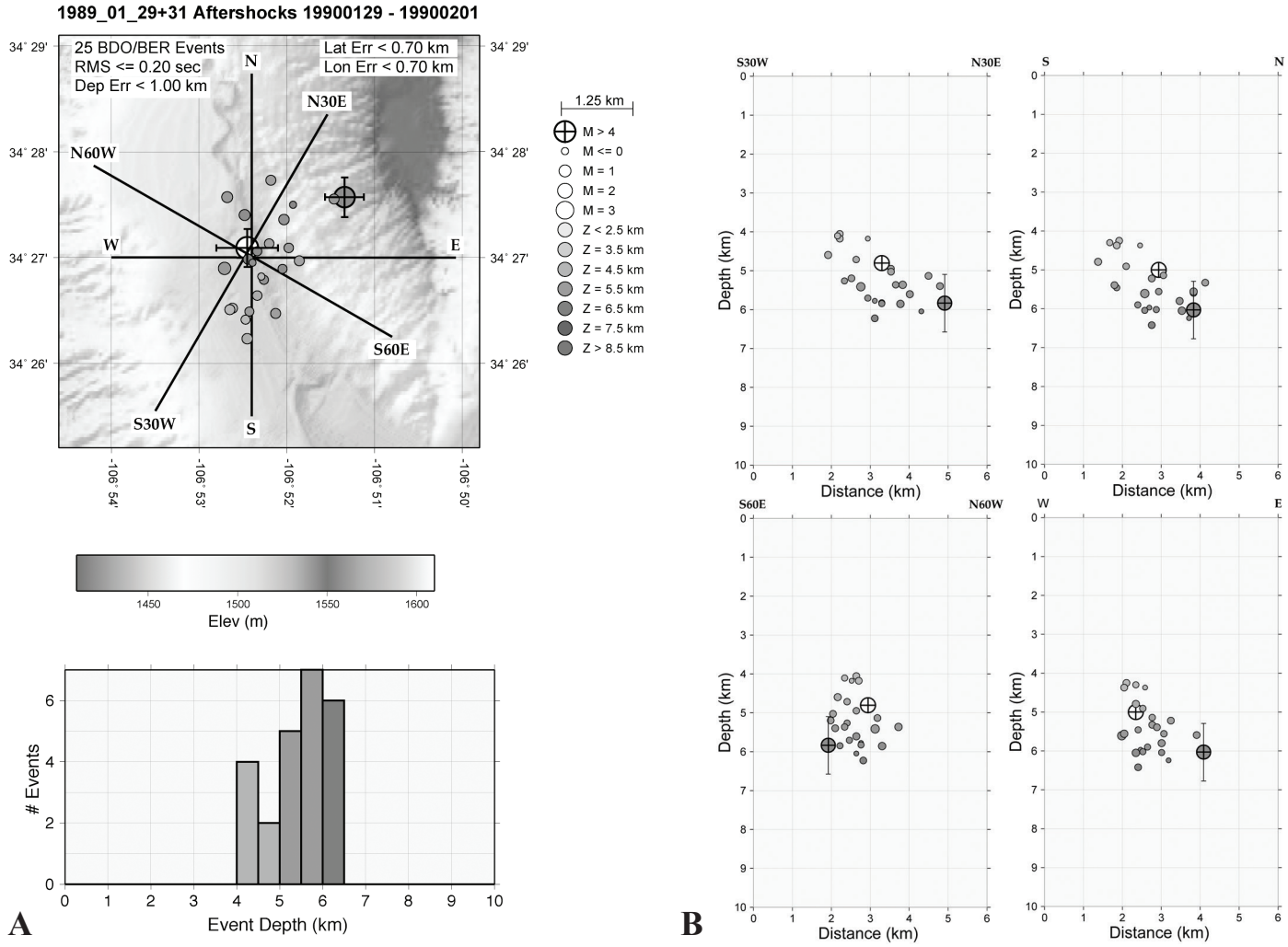

FIGURE 8. Aftershocks (M ≤ 0.7) of the 29 January 1990 M=4.6 earthquake. **A**) Epicenter map and focal depth histogram. **B**) Depth cross-sections. See also Color Plate 11.

The mapped faults near the swarm have west dips (Fig. 3). Therefore, the west-dipping nodal plane for the 29 January 1990 earthquake is the more probable fault plane than the east-dipping nodal plane selected by FPFIT. Considering uncertainties, the strikes for the west-dipping nodal planes are in agreement with the fault orientations obtained by Fan and Wallace (1991) and suggested by the distributions of aftershocks (Figs. 7 and 8).

SEISMIC REFLECTION PROFILES

Two high-resolution seismic reflection profiles pass within less than 3 km to the south and north of the center of the 1989-1991 swarm (Fig. 3). COCORP Line 1A (Brown et al., 1978, and Brown et al., 1980) to the south of the swarm was completed in 1976-1977, and Shell Oil Line 52 to the north was run sometime in the period 1978-1980. Interpretations of COCORP Line 1A (Cape et al., 1983, and deVoogd et al., 1988) and Shell Oil Line 52 (Russell and Snelson, 1994) indicate very complex structure beneath the RGR. Most prominent are major listric faults that are responsible for the east-west extension of the RGR.

A geologic model was developed by deVoogd et al. (1988) for the region along the COCORP profile immediately to the south of the swarm that could replicate the seismic reflection profile (Fig. 11). The outstanding structural feature of the model is an east-dipping listric fault. Located just above this fault is the east-west/depth area occupied by 56 small aftershocks of the swarm with longitude errors of ≤0.42 km and depth errors of ≤0.62 km. There is no evidence on the seismic section for steeply dipping north-south striking faults above the listric fault, nor for any offset of it below the location of the swarm earthquakes. We therefore believe the swarm occurred on minor faults that may be accommodating stresses generated by movements, possibly aseismic, along the listric fault.

DATA INTERPRETATION SUMARY

Time and Magnitude Distribution of 1989-91 Swarm Earthquakes

Richter (1958) defines an earthquake swarm as a "long series of large and small shocks with no outstanding principal

TABLE 2. Information of aftershock studies.

Date	Number of Aftershocks	Depth Error Avg. & (1 s.d.)	Latitude Error Avg. & (1 s.d.)	Longitude Err. Avg. & (1 s.d.)
29 Nov. 1989	32	0.64 (0.13) km	0.58 (0.03) km	0.36 (0.07) km
29 Jan. 1990	22	0.63 (0.12) km	0.58 (0.06) km	0.36 (0.05) km

event." The 1989-1991 sequence certainly matches this definition, with a duration of ~560 days with the four strongest earthquakes of magnitudes 4.7, 4.6, 4.3 and 4.1 (Fig. 4). However, the relationship between number of earthquakes and magnitudes (b-value = 0.57) indicates far fewer small shocks relative to large shocks than expected (Scholz, 1990). Richter (1958) presents mainshock-aftershock data that yield b-values in the range of approximately 0.6 to 1.0. The observation that the 1989-91 swarm's b-value is even at the low end of the range for mainshock-aftershock earthquake sequences suggests a different crustal fault-stress environment exists in this portion of the RGR compared to seismically active geologic areas where swarms have high b-values (Richter, 1958).

Strike and Dip of Fault Movements During the Swarm

Estimates of strike and dip for the two strongest earthquakes in the swarm are available from three studies; the two presented in this paper are based on (1) first-motions and (2) locations of small aftershocks following the strongest earthquakes. The third is a paper by Fan and Wallace (1991), who used data from a single very broadband seismograph to determine that the two strong quakes were the result of movement on two closely spaced, north striking, and moderately dipping normal faults. The hypocenters of the small aftershocks of the two strongest events also support slip on two closely spaced, north-striking faults. The aftershock investigation also indicates that dips are steep, but uncertainties in the strike and dip parameters were not determined.

The first-motion studies indicate that west- or east-dipping fault slip could have occurred. However, the west-dipping nodal plane in the first-motion studies of the M=4.7 and M=4.6 quakes have the most northerly strikes, N20W and N16E, respectively. Also, mapped faults near the swarm area have west dips (Fig. 3). Errors in the strike and dip of the two west-dipping nodal planes permit movement on two closely spaced nearly parallel faults.

Rupture Areas

The estimated rupture areas from the aftershock studies are 4.5 km^2 for the M=4.7 quake and 4.0 km^2 for the M=4.6 quake. Wells and Coppersmith (1994) have established relationships between rupture area and magnitude for strike-slip, reverse, and normal faults and for all fault types combined. The latter has been adopted for a comparison with the 1989-91 rupture areas because it is based on 148 earthquakes, whereas the relationship for normal faults is only based on 22. The Wells and Coppersmith (1994) one standard deviation range in rupture areas are: 3.5 km^2 to 10.6 km^2 for the M=4.7 quake; and 2.9 km^2 to 8.7 km^2 for the M=4.6 quake. Estimates of rupture areas presented in this paper from the aftershock studies fall within these one standard deviation ranges and therefore are considered reasonable.

The Bernardo Swarm and RGR Tectonics

Seismic reflection profiles in the Bernardo area indicate that the major faults accommodating east-west extension of the rift are listric. The prominent listric fault in the Bernardo swarm area is located below the swarm hypocenters. Movement on the listric fault would stress the over-riding crust to the point

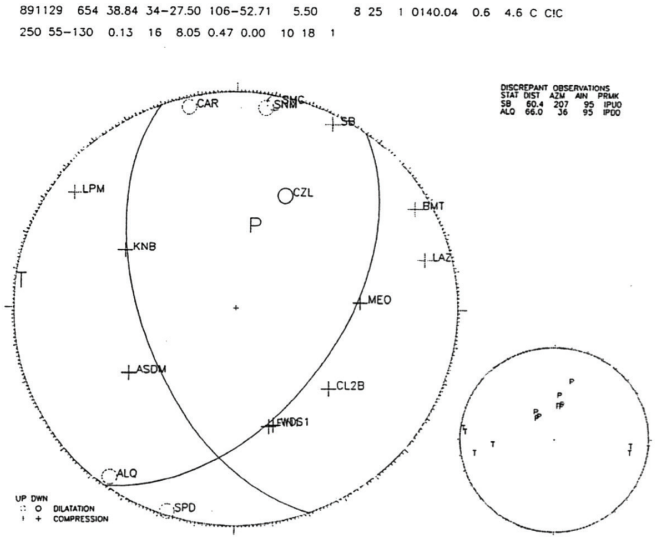

FIGURE 9. FPPLOT diagram of the fault mechanism for the 29 November 1989 M=4.7 earthquake (Reasenberg and Oppenheimer, 1985).

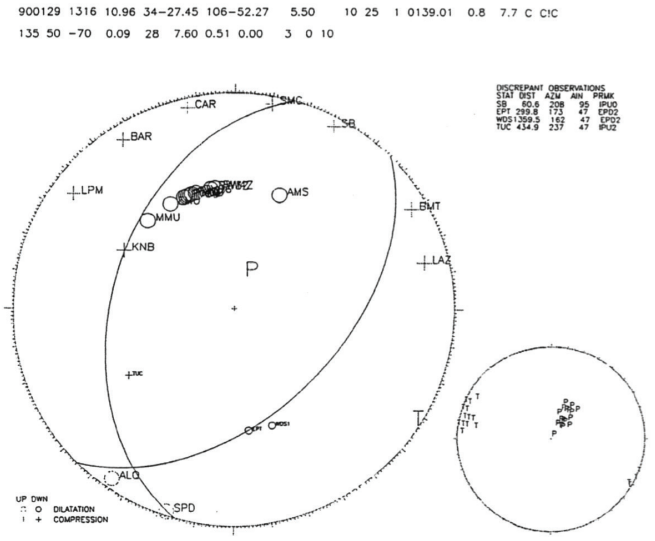

FIGURE 10. FPPLOT diagram of the fault mechanism for the 29 January 1990 M=4.6 earthquake (Reasenberg and Oppenheimer, 1985).

TABLE 3. Focal mechanism solutions for two Bernardo earthquakes.

Date (Yr/Mo/Day)	Time	N[1]	T-axis	Strike (±Err)	Dip (±Err)	Rake (±Err)	Fault Type	Strike (±Err)	Dip (±Err)	Rake (±Err)	Fault Type
89/11/29	06:54	16	275°	340°	55°	-130°	Normal	36°	52°	-50°	Normal
				(10°)	(18°)	(1°)	Rt.Lt.Oblq.				Lft.Lt.Oblq.
90/01/29	13:16	28	300°	16°	45°	-110°	Normal	45°	50°	-70°	Normal
								(3°)	(0°)	(10°)	
			West	Dip	Nodal	Plane		East	Dip	Nodal	Plane

[1]N = number of stations used to estimate focal mechanism

of rupture and thus cause the 1989-1991 Bernardo earthquake swarm. Perhaps the stronger 1906-1907 Socorro swarm (Reid, 1911; Sanford, 2008) may have been generated in the same way.

ACKNOWLEDGMENTS

We thank Garrett Euler and Jonathan Maccarthy at Los Alamos National Laboratory for providing helpful reviews and suggestions that improved this paper. From the New Mexico Bureau of Geology and Mineral Resources, we thank David Love for recommending this paper for the Fall Guidebook, and we especially thank Bonnie Frey for coordinating text and figure edits and Leo Gabaldon for outstanding figure editing.

REFERENCES

Ake, J.P., and Sanford, A.R., 1988, New evidence for the existence and internal structure of a thin layer of magma at mid-crustal depths near Socorro, New Mexico: Seismological Society of America Bulletin, v. 78, p. 1335-1359.

Ake, J.P., Sanford, A.R., and Jarpe, S.J., 1983, A magnitude scale for central New Mexico based on signal duration: New Mexico Institute of Mining and Technology, Geophysics Open-file Report 45, 26 p.

Balch, R.S., Hartse, H.E., Sanford, A.R., and Lin, K.W., 1997, A new map of the geographic extent of the Socorro mid-crustal magma body: Seismological Society of America Bulletin, v. 87, p. 174-182.

Brown, L.D., Chapin, C.E., Sanford, A.R., Kaufman, S., and Oliver, J., 1980, Deep structure of the Rio Grande rift from seismic reflection profiling: Journal of Geophysical Research, v. 85, p. 4773-4800.

Cape, C.D., McGeary, S., and Thompson, G.A., 1983, Cenozoic normal faulting and the shallow structure of the Rio Grande rift near Socorro, New Mexico: Geological Society of America Bulletin, v. 94, p. 3-14.

deVoogd, B., Serpa, L., and Brown, L., 1988, Crustal extension and magmatic processes: COCORP profiles from Death Valley and the Rio Grande rift: Geological Society of America Bulletin, v. 100, p. 1550-1567.

Fan, G., and Wallace, T., 1991, The determination of source parameters for small earthquakes from a single, very broadband seismic station: Geophysical Research Letters, v. 18, p. 1385-1388.

Fialko, Y., and Simons, M., 2001, Evidence for on-going inflation of the Socorro magma body, New Mexico, from Interferometric Synthetic Aperture Radar imaging: Geophysical Research Letters, v. 28, p. 3549-3552.

Hartse, H.E., 1991, Simultaneous hypocenters and velocity model estimation using direct and reflected phases from microearthquakes recorded within the central Rio Grande rift, New Mexico [Ph.D. dissertation]: Socorro, New Mexico Institute of Mining and Technology, 251 p.

Hartse, H.E., Sanford, A.R., and Knapp, J.S., 1992, Incorporating Socorro magma body reflections into the earthquake location process: Seismological Society of America Bulletin, v. 82, p. 2511-2532.

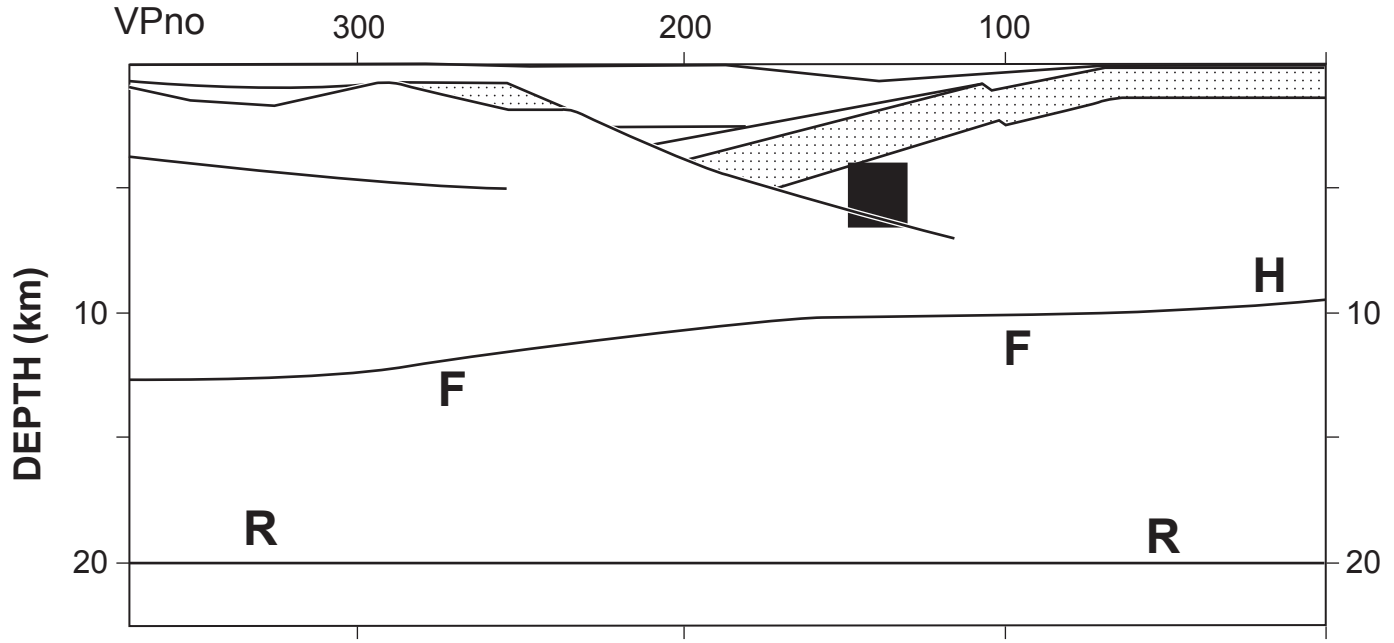

FIGURE 11. Geologic model of the crustal structure by deVoogd et al. (1988), that replicates reflection arrivals on COCORP Line 1A (Brown et al., 1980) (see Fig. 3). The EW/depth distribution of the small aftershock hypocenters is the dark rectangle above the listric fault.

Keller, G., and Baldridge, W., 1999, The Rio Grande rift: A geological and geophysical overview: Rocky Mountain Geology, v. 34, p. 121-130.

Machette, M.N., Personius, S.F., Kelson, K.I., Haller, K.M., and Dart, R.L., 1998, Map and data for Quaternary faults and folds in New Mexico: U.S. Geological Survey, Open-file Report 98-821, 443 p., 1 pl.

Morgan, P., Seager, W.R., and Golombek, M.P., 1986, Cenozoic thermal, mechanical, and tectonic evolution of the Rio Grande rift: Journal of Geophysical Research, v. 91, p. 6263-6276.

Newton, C.A., Cash, D.J., Olsen, K.H., and Homuth, E.F., 1976, LASL seismic programs in the vicinity of Los Alamos, New Mexico: Los Alamos Scientific Laboratory, Informal Report, LA-6406-MS, 42 p.

Reasenberg, R., and Oppenheimer, D.H., 1985, FPFIT, FPPLOT and FPPAGE; Fortran computer programs for calculating and displaying earthquake fault-plane solutions: U.S. Geological Survey Open-file Report 85-739, 109 p.

Reid, H.F., 1911, Remarkable earthquakes in central New Mexico in 1906 and 1907: Bulletin of the Seismological Society of America, v. 1, p. 10-16.

Reilinger, R.E., and Oliver, J.E., 1976, Modern uplift associated with a proposed magma body in the vicinity of Socorro, New Mexico: Geology, v. 4, p. 583-586.

Richter, C.F., 1958, Elementary Seismology: San Francisco, W. H. Freeman, 768 p.

Russell, L., and Snelson, S., 1994, Structure and tectonics of the Albuquerque basin segment of the Rio Grande rift, Insights from reflection seismic data: Geological Society of America, Special Paper 291, p. 39-58.

Sanford, A.R., 2008, New estimates of the magnitudes and locations for the strongest earthquakes in 1906-07 Socorro, New Mexico, earthquake swarm: New Mexico Geology, v.30, p.116-121.

Sanford, A.R., Balch, R.S., and Lin, K.W., 1995, A seismic anomaly in the Rio Grande rift near Socorro, New Mexico: New Mexico Institute of Mining and Technology, Geophysics Open-file Report 78, 18 p.

Sanford, A.R., Lin, K.W., Tsai, I., and Jaksha, L.H., 2002, Earthquake catalogs for New Mexico and bordering areas: 1869-1998: New Mexico Bureau of Geology and Mineral Resources, Circular 210, 104 p.

Sanford, A.R., Mayeau, T.M., Schlue, J.W., Aster, R.C., and Jaksha, L.H., 2006, Earthquake catalogs for New Mexico and bordering areas II: 1999-2004: New Mexico Geology, v. 28, p. 99-109.

Scholz, C.H., 1990, The Mechanics of Earthquakes and Faulting: New York, Cambridge University Press, 439 p.

Wells, D.J., and Coppersmith, K.J., 1994, New empirical relationships among magnitude, rupture length, rupture width, rupture area, and surface displacement, Bulletin of the Seismological Society of America, v. 84, p. 974-1002.

Folds in Estadio Canyon. Photo courtesy of Bonnie Frey.